THE JOURNAL OF BIOLOGICAL CHEMISTRY VOL. 288, NO. 18, pp. 13082–13092, May 3, 2013

Inorganic Pyrophosphatase Defects Lead to Cell Cycle Arrest and Autophagic Cell Death through NAD^+ Depletion in Fermenting Yeast*

Received for publication, November 23, 2012, and in revised form, January 25, 2013 Published, JBC Papers in Press, March 11, 2013, DOI 10.1074/jbc.M112.439349

Gloria Serrano-Bueno[‡1], Agustín Hernández[‡§1,2], Guillermo López-Lluch[¶], José Román Pérez-Castiñeira[‡], Plácido Navas[¶], and Aurelio Serrano[‡3]

From the [‡]Instituto de Bioquímica Vegetal y Fotosíntesis, Universidad de Sevilla-Consejo Superior de Investigaciones Científicas (CSIC), Avda. Américo Vespucio 49, 41092 Seville, Spain, [§]Department of Physiology, Anatomy, and Cell Biology, Universidad Pablo de Olavide, Carretera de Utrera Km 1, 41013 Seville, Spain, and [¶]Centro Andaluz de Biología del Desarrollo, Universidad Pablo de Olavide-CSIC and Centro de Investigación Biomédica en Red de Enfermedades Raras (CIBERER), Instituto de Salud Carlos III, 41013 Seville, Spain

Background: The cellular consequences of inorganic pyrophosphate excess in a eukaryotic cell are unknown.
Results: *Saccharomyces cerevisiae* cells depleted of inorganic pyrophosphatase Ipp1p on respiratory carbon sources undergo cell cycle arrest, but fermenting cells undergo NAD^+ depletion-induced autophagy and die.
Conclusion: Inorganic pyrophosphatase depletion can cause cell death through autophagy.
Significance: This is the first work detailing the cellular consequences of intracellular pyrophosphate accumulation in eukaryotes.

Inorganic pyrophosphatases are required for anabolism to take place in all living organisms. Defects in genes encoding these hydrolytic enzymes are considered inviable, although their exact nature has not been studied at the cellular and molecular physiology levels. Using a conditional mutant in *IPP1*, the *Saccharomyces cerevisiae* gene encoding the cytosolic soluble pyrophosphatase, we show that respiring cells arrest in S phase upon Ipp1p deficiency, but they remain viable and resume growth if accumulated pyrophosphate is removed. However, fermenting cells arrest in G_1/G_0 phase and suffer massive vacuolization and eventual cell death by autophagy. Impaired NAD^+ metabolism is a major determinant of cell death in this scenario because demise can be avoided under conditions favoring accumulation of the oxidized pyridine coenzyme. These results posit that the mechanisms related to excess pyrophosphate toxicity in eukaryotes are dependent on the energy metabolism of the cell.

Many biosynthetic reactions produce inorganic pyrophosphate (PP_i) as a by-product. The advantage of this seems to lie in a greater $\Delta G'^0$ stored in the α,β-phosphoanhydride bond of nucleoside triphosphates compared with that in the β,γ-phosphoanhydride bond and the fact that PP_i is rapidly hydrolyzed to orthophosphate, driving both the kinetics and energetics of anabolic reactions toward biosynthesis (1). For this reason, PP_i homeostasis is exceedingly important for the cell. Removal of PP_i from the cytosol is carried out by two main non-homologous enzyme types: soluble inorganic pyrophosphatases (sPPases)[4] and proton-translocating membrane-bound pyrophosphatases (H^+-PPases) (2, 3). The first of these is found as the sole enzyme that keeps cytosolic PP_i at very low levels in animals and fungi. Soluble PPases may share this function with their membrane-bound counterparts in plants, protists, and some bacteria and archaea; albeit until now only the involvement and proper location of the membrane-bound H^+-PPases have been proved in these organisms (2, 3). Not surprisingly then, a genetic defect leading to the absence of sPPase activity has been found to cause *Escherichia coli* to stop cell proliferation (4) and to be inviable in the budding yeast *Saccharomyces cerevisiae* (5–8). In the case of *E. coli*, this growth defect was shown to be non-lethal (4). However, no study to date has dealt with the physiological basis accounting for the lethality of sPPase deficiency in eukaryotes or how it affects the cell cycle in either prokaryotes or eukaryotes.

Up to now, the cellular importance of PP_i homeostasis has only been patchily and scantily studied. In bacteria, it has been observed that the level of intracellular PP_i does not correlate directly with that of sPPase polypeptide; on the contrary, it remains constant until the amount of this enzyme drops below a minimum threshold (9), suggesting post-translational regulation of its catalytic activity or a constitutive excess of this

* This work was supported by grants from the Andalusian Regional Government and the Spanish Ministries of Science and Innovation and of Health, Social Policies, and Equality (to Plan Andaluz de Investigación, Desarrollo e Innovación Groups BIO-261 and BIO-177) and Grants P07-CVI-3082, BFU2007-61887, BFU2010-15622, FIS-PI080500, and P08-CTS-3988, all of them partially funded by European Regional Development Fund program.
[1] Both authors contributed equally to this work.
[2] To whom correspondence may be addressed: Inst. de Bioquímica Vegetal y Fotosíntesis, Universidad de Sevilla-CSIC, Avda. Américo Vespucio 49, 41092 Seville, Spain. Tel.: 34-954-489500; Fax: 34-954-460065; E-mail: agustin.hernandez@ibvf.csic.es.
[3] To whom correspondence may be addressed. Tel.: 34-954-489500; Fax: 34-954-460065; E-mail: aurelio@ibvf.csic.es.

[4] The abbreviations used are: sPPase, soluble inorganic pyrophosphatase; H^+-PPase, proton-translocating membrane-bound pyrophosphatase; SG, standard glucose (2% glucose); CR, caloric restriction (0.5% glucose); MR, mandatory respiration (3% glycerol); Bicine, *N*,*N*-bis(2-hydroxyethyl)glycine.

enzyme under physiological conditions. In mammals, alteration of sPPase levels is associated to several illnesses, many related to calcium phosphate homeostasis (10, 11). Interestingly, human sPPase PPA1 is now being found associated with tumor cells. Thus, cytosolic levels of this protein have been shown to be increased in several proteomics studies dealing with cancer tissues from different origins, such as lung and colon (12, 13). In addition, plants have a very intricate PP_i metabolism: they possess a number of structurally and catalytically diverse PP_i-utilizing proteins like the membrane-bound H^+-PPases, several PP_i-dependent glycolytic enzymes, and multiple sPPase isoforms (2, 3, 14). It has been observed that photosynthetic carbon assimilation and plant metabolism in general are greatly affected by changes in the levels of soluble PPases (15–17). However, we cannot start to understand plant PP_i metabolism and its influence on economically important issues, such as seed oil or carbohydrate yield, if we are unsure how simpler unicellular organisms behave in this respect.

In this report, we show for the first time that a conditional genetic defect in the yeast *IPP1* gene induces massive cell death in fermenting cultures but only induces cell cycle arrest in respiring cells. Furthermore, we describe the physiological mechanism for cell death and the metabolic step that causes it. In addition we show that under respiratory conditions cell cycle arrest is reversible. These results may open the way to new approaches in metabolism-related cell bioengineering and chemotherapy and underline the importance of so-called housekeeping cell processes like PP_i homeostasis.

EXPERIMENTAL PROCEDURES

Yeast Strains, Plasmids, and Growth Conditions—All *S. cerevisiae* strains are derivatives of W303-1a (MATa *leu2-3,112 trp1-1 can1-100 ura3-1 ade2-1 his3-11,15*) or SEY6210 (MATα *leu2-3,112 ura3-52 his3-*Δ*200 trp1-*Δ*901 lys2-801 suc2-*Δ*9 GAL*). Relevant genotypes are as follows: YPC3, W303-1a *ipp1*$_{UAS}$::*GAL1*$_{UAS}$*-IPP1-HIS3* (18); SAH6, *YPC3 vph1*Δ::*KanMX4*; SAH16, SEY6210 *ipp1*$_{UAS}$::*GAL1*$_{UAS}$*-IPP1-HIS3*; SAH17, *SAH16 atg8*Δ::*LEU2*. A multicopy plasmid bearing *NQR1* under the control of the *ADH1* promoter and its empty parental plasmid were kind gifts of Dr. Carlos Santos-Ocaña and have been described (19). Introduction of plasmids into yeast cells was done by the lithium acetate method (20). Cells were routinely grown on standard YP medium (1% yeast extract, 2% peptone) supplemented with appropriate carbon sources. Unless otherwise stated, all determinations were done on exponentially growing cells (A_{600} of cultures not greater than 0.5). To maintain cultures for several hours below an A_{600} of 0.5, they were routinely diluted with fresh medium every 2–3 h until the end of the experiment (semicontinuous culture). In experiments where a single time point was assayed, all determinations were done on cells incubated for 18 h under standard glucose (2% glucose) (SG) or caloric restriction (0.5% glucose) (CR) condition or for 36 h under mandatory respiration (3% glycerol) (MR) condition unless indicated otherwise. Nitrogen starvation conditions were induced by incubating cells for 6 h in 0.17% yeast nitrogen base without amino acids or ammonium sulfate and supplemented only with 2% galactose. No loss in viability due to these starvation conditions was observed as assessed by colony-forming unit (cfu) counting.

Cell Death and Viability Assays—Cell viability was assessed by colony forming ability. Briefly, approximately 500 cells as estimated by A_{600} were plated onto the appropriate solid medium, and survival was scored as the percentage of colonies formed from the total inoculated cells. Because different conditions could lead to alterations in the number of yeast cells estimated by absorbance due to size differences, estimations were corrected by counting cells on a hemocytometer. Death was estimated on propidium iodide-stained cells by flow cytometry as cells bearing DNA contents less than 1C (sub-G_1) (21).

Flow Cytometry and Microscopy—Cells were stained with propidium iodide essentially as described by Sazer and Sherwood (22) and analyzed on a Coulter Epics XL apparatus as described (23).

For microscopical analysis, cells were visualized using a Leica DM 6000B type fluorescence microscope. Cell size was evaluated from differential interference contrast microphotographs as the apparent area covered by the cell evaluated using the NIH ImageJ program (24). Percentages of budded cells were estimated from microphotographs; a minimum of 150 cells per treatment were counted. TUNEL assays were done essentially as described (25) using a commercial kit (Roche Applied Science, catalog number 11684817910). Cells were stained by incubating with 5 μg/ml dihydrorhodamine 123 for 2 h under appropriate growth conditions and then viewed under a rhodamine filter. FM4-64 staining was done as described (26); estimation of the percentage of cells showing solid vacuoles on FM4-64 staining was done as for budded cells above.

Cell Extracts and Enzymatic Assays—Cytosol-enriched fractions were obtained from exponentially growing cells by breaking them using glass beads (0.5-mm inner diameter) in a buffer containing 0.33 M sorbitol, 25 mM Tris-HCl (pH 7.5), 2 mM EDTA, 2 mM DTT, 1 mM PMSF, 1 mM benzamidine, and 1 mM ϵ-aminocaproic acid. Cells were subjected to five 1-min bursts on a Vortex mixer at full speed with 1-min intervals on ice between bursts. Total homogenates were cleared of unbroken cells and cell debris by low speed centrifugation (5 min at 500 $\times$ *g*) followed by high speed centrifugation for 15 min (20,000 $\times$ *g*). The pyrophosphatase activity assay was performed as described previously (8), and released phosphate was determined as described (27). Activity in the presence of 2 mM potassium fluoride, corresponding to unrelated diphosphatase activities, was subtracted from the data. These activities represented less than 5% of total PP_i hydrolytic activity measured in control cells.

Protein Determination and Western Blotting—Protein determination was done using a dye binding-based assay from Bio-Rad (catalog number 500-0006) according to the manufacturer's instructions and using ovalbumin as a standard. Proteins were separated by SDS-PAGE using standard procedures. Proteins were then transferred to nitrocellulose filters and probed with antibodies raised against the sPPase PPA I from the microalga *Chlamydomonas reinhardtii* (14) or a commercial anti-GFP antibody (Clontech, catalog number 632460). Proteins were visualized on x-ray films using horseradish peroxi-

dase-coupled secondary antibodies and a chemiluminescence kit (Millipore, catalog number WBKLS0100).

Quantitation of Metabolites—For PP_i quantitation, YPC3 cells were grown on the appropriate medium for 24 h under semicontinuous culture conditions as stated above. Approximately 10^9 cells were collected by centrifugation, washed with ice-cold water, and extracted with 1 ml of 4% perchloric acid. To aid cell breakage, cells were subjected to three 1-min Vortex bursts in the presence of glass beads (0.5-mm inner diameter). After decanting glass beads and debris by centrifugation, extracts were neutralized by adding sequentially 140 μl of 5 M KOH and 60 μl of 1 M Tris-HCl (pH 7.5) and centrifuged again at top speed in a tabletop centrifuge for 30 min to decant potassium perchlorate salts. PP_i was measured in the supernatants using a commercial kit (Molecular Probes, catalog number E-6645) according to the manufacturer's instructions. Pyridine nucleotide coenzyme extractions were performed as follows. Briefly, YPC3 and W303-1a cells were grown under semicontinuous conditions for 18 h (SG and CR conditions) or 36 h (MR and galactose controls). Then approximately 2.5×10^7 cells were washed with ice-cold water, resuspended in 200 μl of either 50 mM NaOH (NADH extraction) or 50 mM HCl (NAD^+ extraction), and heated at 60 °C for 30 min on a heat block. After this, extracts were neutralized and clarified by centrifugation. Coenzymes were determined using a coupled assay consisting of 10 mM Bicine, pH 8.0, 15 units/ml yeast alcohol dehydrogenase (Sigma-Aldrich, catalog number A-7011), 0.4 mg/ml phenazine methosulfate, 0.25 mg/ml thiazolyl blue formazan, and 3% ethanol. Pyridine nucleotide coenzyme levels were spectrophotometrically estimated at 570 nm as the kinetic production of reduced formazan.

RNA Methods—Yeast RNA was extracted using the hot phenol method (28). One microgram of RNA was subjected to cDNA synthesis using a Quantitect reverse transcription kit (Qiagen, catalog number 205311) according to the manufacturer's instructions. PCR was done using 1 μl of newly synthesized cDNA in a 20-μl tube. Sequences of the oligonucleotides used as primers are available upon request. The total number of cycles was set to 25 to avoid saturation. Amplified DNA was separated on agarose gels under standard conditions, photographed using a Gel Doc XR+ System (Bio-Rad, catalog number 170-8195) and quantified using Quantity One v4.6.2 software (Bio-Rad, catalog number 170-9600).

Miscellaneous Methods—Experiments were typically done in triplicate. The actual number of independent experiments is included in the figure legends (n). When data from representative experiments are shown, this is stated in each case. Statistical analysis was done using unpaired t tests with a cutoff of $p \leq 0.05$.

RESULTS

Effect of Ipp1p Deficiency on Cell Viability—We have previously shown that a *S. cerevisiae* engineered strain in which the gene *IPP1* encoding its cytosolic sPPase is governed by a *GAL1* inducible/repressible promoter (8) is viable as long as a plasmid-borne heterologous H^+-PPase is expressed when the *GAL1* promoter is repressed. An improved version of this mutant (YPC3) (18) has been used to study the kinetics of events related to Ipp1p deficiency to delineate the cellular importance of PP_i homeostasis. Phosphate and carbon metabolisms are long known to interact in their regulation (for example, see Ref. 29). Also, viability is increasingly associated to carbon source quality and availability in many organisms, in particular to the dichotomy between fermentation and respiration and more recently to calorie availability (30–32). Having this in mind, we compared YPC3 control cells (grown on *GAL1*-inducing conditions, 2% galactose) with others placed under three different repressing carbon source conditions: SG, CR, and MR. As expected, after 24 h, YPC3 cells accumulated 0.31 ± 0.05, 0.31 ± 0.05, 0.21 ± 0.02, and 0.02 ± 0.01 nmol of $PP_i/10^6$ cells in SG, CR, MR, and galactose control conditions, respectively; *i.e.* SG and CR cells displayed approximately 16-fold and MR cells displayed approximately 10-fold greater levels of PP_i than those observed under galactose conditions. On the other hand, Ipp1p polypeptide levels decreased sharply upon switch of YPC3 cells from galactose (control) to glucose irrespective of its concentration (Fig. 1*A*, SG and CR). In addition, the switch to MR conditions induced a slower rate of Ipp1p disappearance. This is in agreement with the *GAL1* promoter being inactive due to the lack of its transcription factor, *Gal4p*, when cells are grown on this carbon source but not actively repressed by *Gal80p* and *Mig1p* as it is under glucose conditions (33). In any case, Ipp1p polypeptide levels were undetectable on Western blots 6 h after the switch to glucose and 24 h after the switch to MR. These results were confirmed by PP_i hydrolytic activity assays (Fig. 1*B*). Six hours after the switch to SG or CR or 24 h after the switch to MR, no sPPase activity was observed. Concomitant with this, growth was slowed to a halt after 18 h under SG and CR conditions and 36 h under MR condition (Fig. 1*C*), whereas galactose controls showed a constant growth rate even after 48 h of semicontinuous culture.

To ascertain whether viability was compromised and the stage of sPPase activity at which this reduction occurs, we also followed the ability of these cells to form colonies (Fig. 1*D*). Albeit enzymatic activity was undetectable much earlier, cell viability was not observed to drop until 18 h after switching to SG or CR condition, and after 21 h, it was observed to plateau and reach a minimum at approximately 27% of plated cells. Similarly, the viability of MR cells dropped severely at 36 h and reached the same lowest value as SG and CR cells after 48 h (Fig. 1*D*). In subsequent experiments where only a single time point was assayed, unless otherwise indicated, all determinations were done on YPC3 cells incubated for 18 h under SG or CR condition or for 36 h under MR condition.

Effect of Ipp1p Deficiency on Cell Cycle—We were interested in determining the consequences that a defect in PP_i homeostasis had on the cell cycle. To this end, we compared the cell cycle profiles of cells incubated under control, SG, CR, and MR conditions (Fig. 2*A*, *left panel*). In this case, a differential behavior was evident between fermenting and respiring cells. Under both fermenting conditions (SG and CR) cells arrested their cycle abruptly; additionally, a great proportion of cells showed a DNA content smaller than that corresponding to a haploid intact genome (sub-G_1), indicative of cell death (21). Conversely, MR cells showed no accumulation of sub-G_1 cells

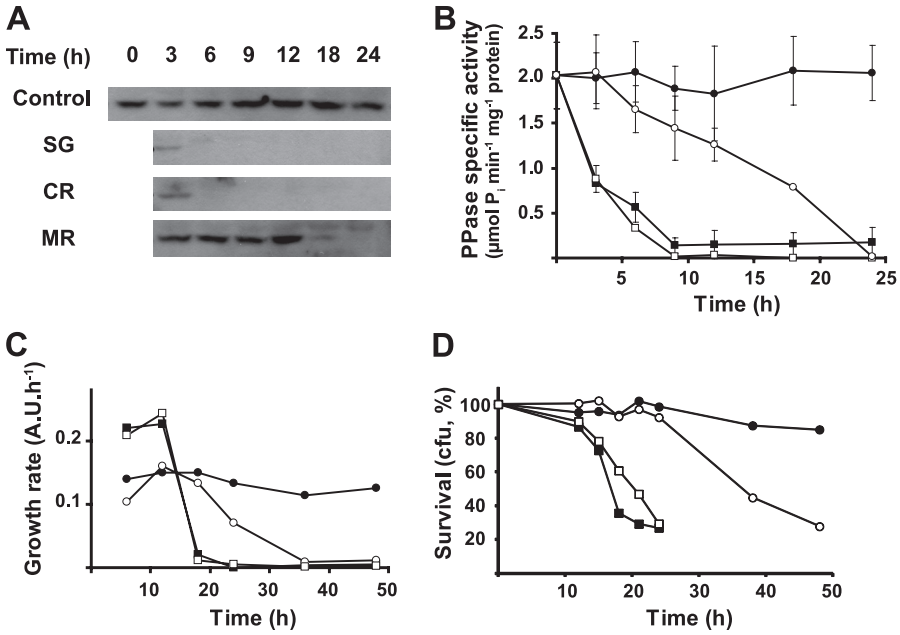

FIGURE 1. **Depletion of Ipp1p sPPase in yeast YPC3 strain as a function of carbon source and time.** *A*, time course of Ipp1p depletion. Levels of Ipp1p polypeptide were evaluated by Western blot. Each lane was loaded with 50 μg of protein from a total cell lysate and probed with an antibody raised against an sPPase from *C. reinhardtii* (see "Experimental Procedures"). *B*, time course depletion of PPase enzyme activity. Whole cell lysates were assayed for phosphate release activity from PP_i as indicated under "Experimental Procedures." *Error bars* denote S.E. ($n = 3$). *C*, changes in growth rates for YPC3 cells maintained in liquid culture. Velocities were estimated as the increment in A_{600}/unit of time. A representative experiment is shown ($n = 2$). *D*, survival ability of YPC3 strain measured as the capacity to form individual colonies (cfu) as a function of carbon source and time ($n = 3$). Maximal values (100%) correspond to 563, 482, 478, and 523 colonies for control, SG, CR, and MR, respectively. For *B*, *C*, and *D*, *solid circles*, 2% galactose control (*Control*); *open circles*, MR condition; *solid squares*, SG condition; *open squares*, CR. *A.U.*, absorbance units.

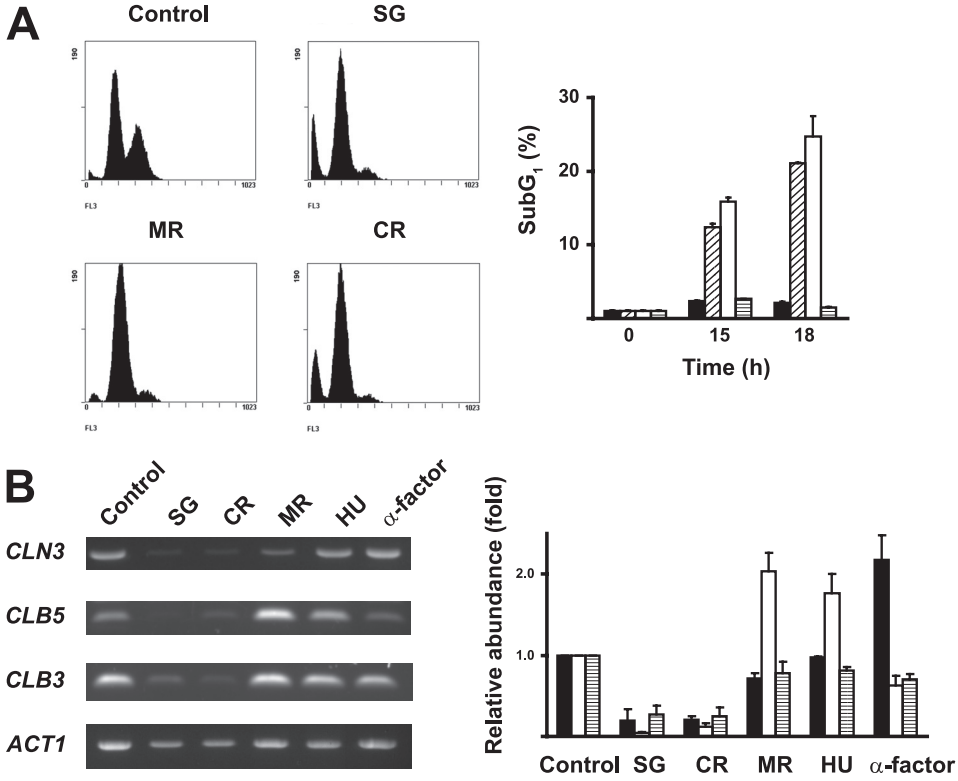

FIGURE 2. **Effects of Ipp1p depletion on cell cycle.** *A*, cell cycle profiles. *Left panel*, propidium iodide flow cytometry histograms of YPC3 cells. YPC3 yeast cultures were kept in galactose (*Control*), SG (for 18 h), CR (for 18 h), or MR (for 36 h) condition at $A \leq 0.5$ prior to analysis. *Right panel*, quantification of sub-G_1 populations from histograms on the *right*. *Solid bar*, control; *oblique hash*, SG; *open bar*, CR; *horizontal hash*, MR. Ten thousand cells were analyzed in each case. *Error bars* denote S.E. ($n = 3$). *B*, cyclin levels in YPC3 cells as a function of energy metabolism. *Left panel*, semiquantitative RT-PCR products obtained using 1 μg of total RNA. *Right panel*, quantification of cyclin abundance on the *left* normalized using *ACT1* as a standard. Maximal values (100%) correspond to 69.5, 35.4, 33.3, and 61.4 arbitrary units for *CLN3*, *CLB5*, *CLB3*, and *ACT1*, respectively. The identity of samples is the same as in *A*. Hydroxyurea (*HU*), 0.1 M for 2 h; α-factor, 10 μg/ml for 2 h. *Solid bars*, *CLN3*; *open bars*, *CLB5*; *hashed bars*, *CLB3*. For both panels, *error bars* denote S.E. ($n = 4$).

despite displaying a nearly equally severe cell cycle arrest. In the case of SG and CR, a discernible sub-G_1 population increase over control cells could be observed as early as 18 h after the carbon source switch (Fig. 2*A*, *right panel*) and reached up to 25% of the cells in a culture. However, under MR conditions, no meaningful increase in the proportion of sub-G_1 cells with respect to control cells was observed even 56 h after the glycerol switch (6.5 ± 1.3 and 2.2 ± 0.2% for MR and control cells, respectively; $n = 10{,}000$ cells). Because propidium iodide staining does not provide enough accuracy to discern between a G_1 and an S phase cell cycle arrest by flow cytometry in budding yeast, we measured the amounts of *CLN3*, *CLB5*, and *CLB3* cyclin mRNAs by semiquantitative RT-PCR as markers of G_1, S, and G_2 phases of the yeast cell cycle, respectively (Fig. 2*B*). Both SG and CR conditions showed a marked depletion of all cyclins studied, a situation usually associated to G_0 (32). MR cells displayed an accumulation of *CLB5* cyclin mRNA and an overall profile similar to that observed in hydroxyurea-treated cells, indicative of S phase arrest, and in sharp contrast to the profile observed in cells where G_1 arrest was induced by addition of α-factor (Fig. 2*B*, *right panel*).

Morphology and Characteristics of Ipp1p-deficient SG and CR Cells—In agreement with cyclin mRNA results, under the microscope (Fig. 3*A*), most MR cells showed large buds compared with control cells (percentages of budded cells ±S.D. from a representative experiment were 46.1 ± 5.9 and 72.2 ± 5.8% for galactose control and MR, respectively; $n = 2$), whereas SG and CR cells were largely unbudded (5.0 ± 3.1 and 5.0 ± 5.2% for SG and CR, respectively). Strikingly, they also showed a characteristic morphology: they were much bigger than control or MR cells and appeared to contain an enlarged vacuole that filled much of the cell interior. When the apparent cellular area observable under the microscope was quantified, MR and control cells showed no statistically significant differences between themselves, whereas SG and CR cells were approximately 2-fold larger than controls (Fig. 3*A*, *bottom panel*). Nuclear DNA degradation and hence large sub-G_1 populations are characteristic features of apoptosis. In this case, nuclear DNA degradation frequently gives rise to the appearance of a characteristic laddering on genomic DNA agarose gels due to internucleosomal fragmentation. However, when genomic DNA from SG and CR cells was electrophoresed, a continuous smear was observed instead (Fig. 3*B*). TUNEL assays were also negative on SG, CR, and MR cells (data not shown). Reactive oxygen species are also typical inducers and markers of programmed cell death (34). However, both SG and CR cells did not show any discernible increases in reactive oxygen species as measured by dihydrorhodamine 123 fluorescence (Fig. 3*C*). In marked contrast, MR cells showed a clear fluorescent staining indicative of reactive oxygen species accumulation; this feature was not observed on the parental W303-1a strain grown under the same conditions.

The prevalence of vacuolization in SG and CR cells led us to test whether autophagy was induced. To test this hypothesis, a *GFP-ATG8* fusion construct was transformed into YPC3, and the proteolytic processing of ATG8 was followed by Western blot as a marker of autophagy. Control cells kept in galactose and MR cells did not show any processing of the GFP-Atg8p

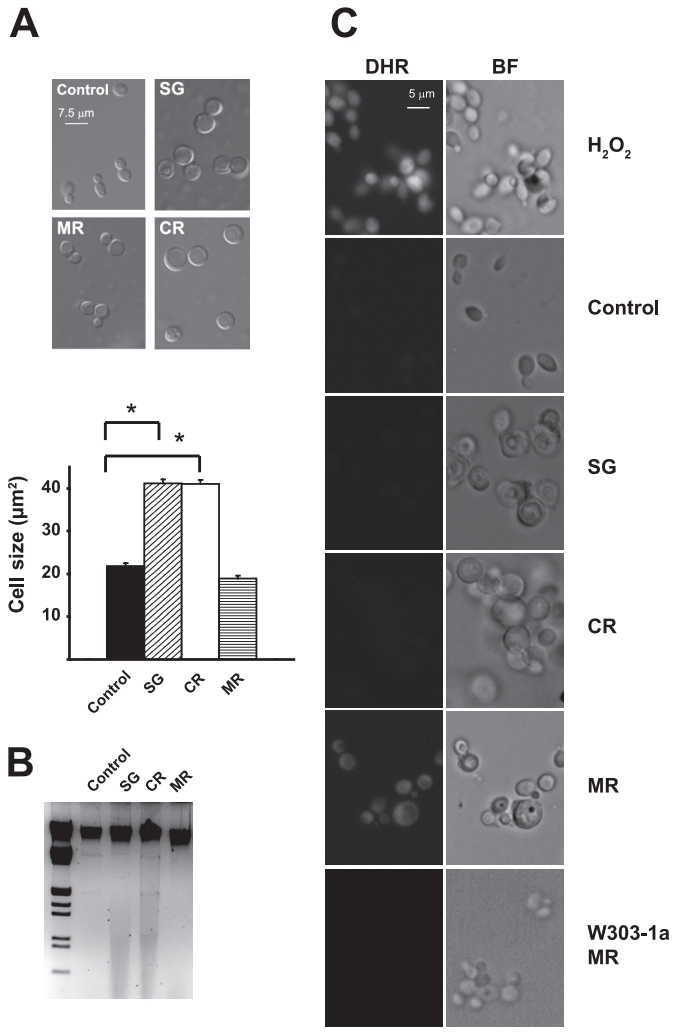

FIGURE 3. **Major cell biological effects of Ipp1p sPPase depletion in YPC3.** *A*, *left panel*, morphology of YPC3 cells as a function of energy metabolism. *Right panel*, quantitation of apparent cell size as the area observed under the microscope. *Solid bar*, control; *oblique hash*, SG; *open bar*, CR; *horizontal hash*, MR. *Error bars* denote S.E. ($n = 3$). *Asterisks* denote significant statistical differences ($p \leq 0.05$). *B*, electrophoresis of genomic DNA obtained from YPC3 cells under different metabolical conditions. Each lane corresponds to 25 μg of DNA; *leftmost lane*, λ DNA digested with EcoRI and HindIII as a size standard. *C*, reactive oxygen species accumulation in YPC3 cells. The presence of reactive oxygen species was evaluated using dihydrorhodamine 123. Cells were stained with 5 μg/ml for 2 h under appropriate growth conditions and then viewed under a rhodamine filter. Oxygen peroxide controls were done by subjecting YPC3 cultures to 1 mM H_2O_2 for 3 h. All cells are YPC3 except where indicated otherwise. *DHR*, dihydrorhodamine 123 fluorescence; *BF*, bright field microscopy.

fusion, whereas SG and CR cells showed a clear band corresponding to liberated GFP in addition to the full fusion. Also, bands of intermediate molecular weight were visible, probably reflecting partial degradation of GFP-Atg8p (Fig. 4*A*). A similar band pattern was displayed by a nitrogen starvation positive control of autophagy.

The fluorescent vital dye FM4-64 has been shown to stain differentially the acidic vacuoles of autophagic yeast cells due to accumulation of membrane material (26). When FM4-64 was added to cultures of SG and CR cells, a pattern of solid vacuoles was observed, similar in appearance to what is observed in nitrogen-starved yeast cells (Fig. 4*B*). The proportion of cells showing solid vacuoles under these conditions was similar to

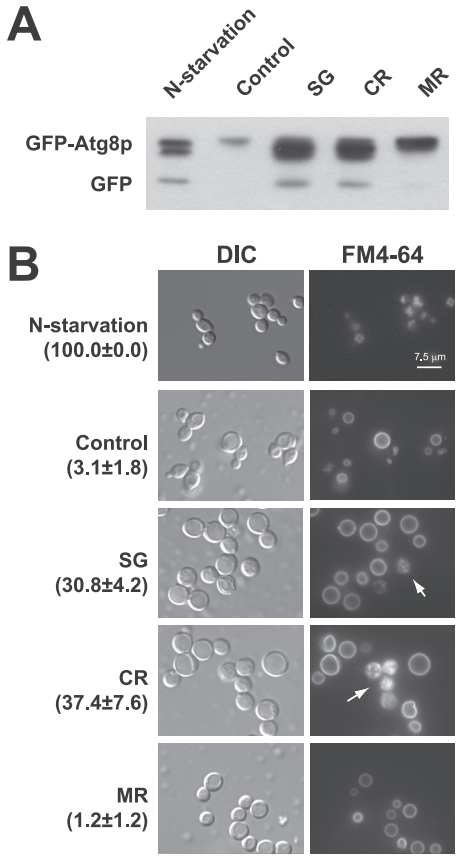

FIGURE 4. **Autophagy in Ipp1p-depleted YPC3 cells.** *A*, processing of a GFP-Atg8p translational fusion. Shown is a Western blot of YPC3 whole cell extracts probed with a commercial antibody recognizing GFP. *B*, accumulation of autophagosomes in YPC3 vacuoles. Acidic compartments were stained using the red fluorescent vital dye FM4-64 (Calbiochem, catalog number 574799). Cells were incubated under SG, CR, or MR condition for 18 (SG and CR) or 36 h (MR) and later stained with the vital dye FM4-64 to display acidic compartments. *DIC*, differential interference contrast; *FM4-64*, fluorescence of FM4-64. *Numbers* in *parentheses* denote the percentage of cells showing solid vacuoles ±S.D. in a representative experiment ($n = 3$). *Arrows* denote autophagic vacuoles.

that of cells bearing sub-G_1 amounts of DNA. On the contrary, galactose-grown control and MR cells did not show any apparent accumulation of FM4-64 inside vacuoles and retained a normal morphology.

Reversibility of Cell Cycle Arrest in MR Cells—In contrast to SG and CR cells, yeast under MR did not show any signs of cell death. We therefore tested whether these cells were in fact arrested in a reversible way and whether removal of excess PP_i could promote recovery. We first tested whether cells grown under MR conditions for 48 h and then placed in fresh YPGalactose liquid medium could resume growth. Indeed, although cells maintained under MR conditions (fresh YPGlycerol medium) could not proliferate, A_{600} clearly increased in YPGalactose cultures (Fig. 5*A*). Nevertheless, these cultures showed an approximately 6-h lag phase. Probably, during this period MR cells lost their cytosolic PP_i due to diffusion and had their *GAL1* promotors released from repression (Fig. 5*A*). We also tested whether the capacity for producing colonies was restored. Cells kept under MR conditions for 48 h that were placed in a releasing liquid medium (YPGalactose) prior to plating on galactose-containing agar plates increased their capacity

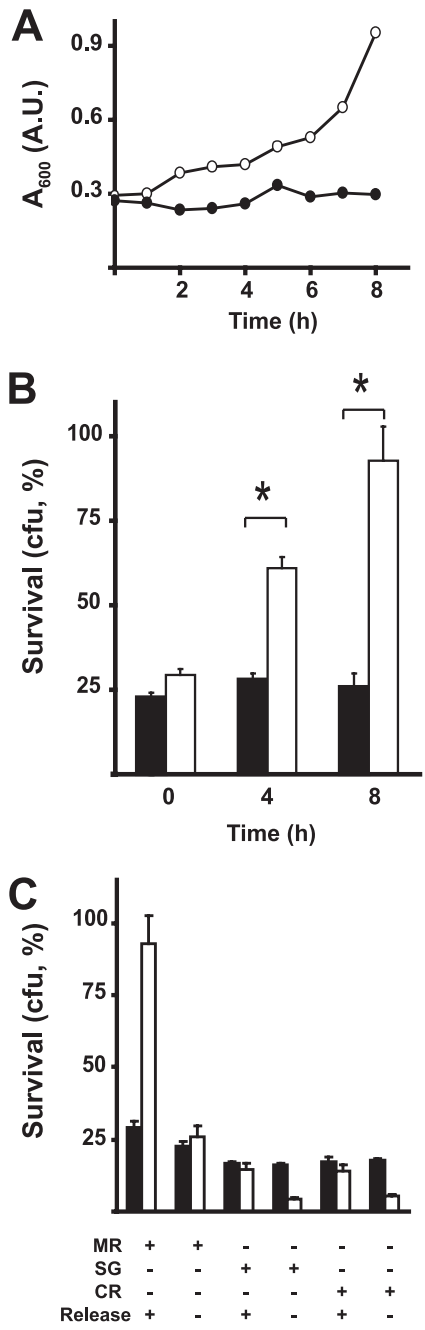

FIGURE 5. **Reversibility of cell cycle arrest in Ipp1p-depleted MR yeast cells.** *A*, growth of MR YPC3 cells in fresh medium. YPC3 cells were kept under MR condition for 48 h and later inoculated into fresh complete medium supplemented with a carbon source as stated below at the indicated A_{600}. Culture turbidity was monitored for 8 h. *Solid circles*, 3% glycerol; *open circles*, 2% galactose. *B*, ability to form individual colonies of cells released in liquid medium. YPC3 cells kept under MR condition for 48 h were later incubated in fresh complete medium supplemented with 2% galactose (*open bars*) or 3% glycerol (*solid bars*) for the indicated times. Survival of cells grown on 2% galactose and later refreshed again in galactose medium for the duration of the experiment (mock) was considered 100% (357 colonies). *Asterisks* denote significant statistical differences ($p \leq 0.05$). *C*, irreversibility of cell cycle arrest under glucose conditions. YPC3 cells were kept under control (2% galactose), SG, CR, and MR conditions for 24 (SG and CR) or 48 h (MR) prior to being inoculated into fresh complete medium identical to the initial medium (−release) or supplemented instead with 2% galactose (+release). After the indicated times, the ability to form individual colonies was tested. Survival of cells grown on 2% galactose and later refreshed again in galactose medium for the duration of the experiment (mock) was considered 100% (380 colonies) *Closed bars*, 0 h in release medium; *open bars*, 8 h in release medium. For all panels, *error bars* denote S.E. ($n = 3$). *A.U.*, absorbance units.

to form colonies in a time-dependent manner as opposed to those kept in YPGlycerol (Fig. 5*B*). This recovery was exclusive of cells that had been subjected to MR conditions. When cells under the SG or CR condition were subjected to an 8-h release in fresh YPGalactose medium, no recovery was observed in their colony forming capacity (Fig. 5*C*).

Molecular Mechanisms Causing Cell Death under SG and CR Conditions—Yeast fermentative metabolism is stoichiometrically taut in regard to NAD^+/NADH homeostasis. Because NAD^+ biosynthetic enzymes have long been known to be sensitive to excess PP_i (35), we hypothesized that the cell levels of pyridine nucleotide coenzymes could be affected in YPC3 cells under SG, CR, and MR conditions. Indeed, levels of NAD^+ dropped significantly in YPC3 cells grown for 18 h under SG and CR conditions and for 36 h under MR condition compared with a parental strain grown in the same conditions (Table 1). Concomitantly, YPC3 cells showed decreased NAD^+/NADH ratios with respect to wild-type cells when grown under SG and CR conditions. Strikingly, YPC3 MR cells displayed an NAD^+/NADH ratio close to that observed in wild-type cells under the same conditions; this is due to a reduction in the levels of NADH that is not observed under SG or CR condition. Depletion of cellular NAD^+ levels has been described to induce massive autophagy and cell death in mammalian cells (36). To test whether such a mechanism was responsible for the induction of cell death in YPC3 yeast cells under SG and CR conditions, we supplemented the growth culture medium with 10 mM acetaldehyde so that yeast cells could oxidize additional amounts of NADH independently from fermentation. Under these conditions, CR cells showed a 3-fold increase in colony forming capacity, reaching levels close to those found for control cells (Fig. 6*A*, *top panel*). Cells kept under SG condition showed a similar behavior (16.3 ± 0.3 and 63.0 ± 3.5% for untreated and acetaldehyde-treated cells 18 h after medium switch, respectively). This effect was accompanied by a drastic reduction in the percentage of cells displaying sub-G_1 characteristics as well as a cell size that was indistinguishable from cells kept in galactose (Fig. 6*A*, *middle* and *bottom panels*, respectively). Moreover, this pattern was repeated in cells transformed with an expression plasmid carrying the ORF of the gene *NQR1* encoding a plasma membrane-bound NADH oxidoreductase (19). Cells overexpressing this enzyme oxidize greater amounts of NADH under fermenting conditions in a coenzyme Q-dependent but alcohol dehydrogenase-independent manner. Yeast YPC3 cells transformed with this construct and subjected to caloric restriction conditions again showed clear differences in survival rate, proportion of cells in sub-G_1, and cell size (Fig. 6*B*, *top*, *middle*, and *bottom panels*, respectively). However, under SG, cells displayed smaller differences despite the overexpression of *NQR1* (survival figures were 54.4 ± 2.3 and 68.4 ± 3.0% for empty plasmid-bearing and NQR1-overexpressing cells 18 h after medium switch, respectively).

Cell Death Process under SG and CR Conditions—Autophagy has been shown to be a cellular process that under certain circumstances can lead to cell death (37). We investigated the involvement of autophagy in the cell death induction and execution taking place under SG and CR conditions. To ascertain whether autophagy was a cause of death and not simply a concomitant process, we made use of two YPC3-derived yeast strains affected in their capability to complete autophagy. Strains defective for *ATG8* are unable to promote the formation of the autophagosome (38). We also deleted *VPH1*, an essential subunit of the vacuolar V-ATPase; this H^+ pump is required for vacuolar acidification and was early shown to be paramount for completion of the autophagic process (39). Cells that had their *IPP1* gene under the control of *GAL1* promoter and devoid of Atg8p or vacuolar V-ATPase activity showed no loss of viability when placed under SG conditions as measured by their capacity to form colonies (Fig. 7, *A* and *B*, *top panels*). Furthermore, they showed dramatic decreases in sub-G_1 cells under flow cytometry (Fig. 7, *A* and *B*, *middle panels*), and the cell size was reduced to almost control levels when compared with galactose-grown control cells (Fig. 7, *A* and *B*, *bottom panels*). Similar results were obtained under CR conditions (survival figures were 42.5 ± 3.2 and 88.9 ± 7.0% for wild-type and *atg8*Δ cells 18 h after medium switch, respectively, on the one hand and 17.2 ± 3.9 and 111.8 ± 6.3% for wild-type and *vph1*Δ cells 18 h after medium switch, respectively, on the other hand).

TABLE 1
Pyridine nucleotide coenzyme contents in yeast cells grown on different carbon sources
Data are shown in μmol/10^6 cells.

	2% galactose	2% glucose	0.5% glucose	3% glycerol
W303-1a				
NAD^+	1.51 ± 0.28	1.28 ± 0.21	1.38 ± 0.18	1.51 ± 0.29
NADH	1.17 ± 0.26	0.49 ± 0.06	0.35 ± 0.04	0.71 ± 0.10
NAD^+/NADH	1.30	2.58	3.94	2.09
YPC3				
NAD^+	1.85 ± 0.25	0.72 ± 0.12[a]	0.71 ± 0.11[a]	0.54 ± 0.11[a]
NADH	1.39 ± 0.18	0.43 ± 0.07	0.31 ± 0.04	0.28 ± 0.05[a]
NAD^+/NADH	1.32	1.67	2.26	1.92

[a] Statistically significant differences compared with W303-1a cells as evaluated by *t* tests ($n = 3$).

DISCUSSION

Despite intensive research, no thorough information yet exists regarding the cellular implications of some basic metabolic processes. One such field is PP_i metabolism. Despite PP_i being involved in pathophysiological bone resorption, suspected to play a role in cancer, and on the whole assumed to affect nearly all aspects of cell anabolism, the effects an alteration of PP_i homeostasis has at the cellular level are still unknown. Although eukaryotes and bacteria present obvious differences, the scant information available from studies in *E. coli* is assumed to hold true for eukaryotes. As a result, it is generally considered that an excess of PP_i would stop cell growth due to an overall inhibition of anabolism and that this situation would be reversible upon PP_i removal from the cell (4). The present work depicts a very different scenario in eukaryotic cells. In yeast, depletion of cytosolic sPPase activity brings cell death but only in the case of cells that obtain their energy from fermentation. This cell death is accompanied by cell cycle arrest in the G_1/G_0 phase, and both cell death induction and cell cycle arrest are irreversible.

The vast majority of the PP_i-producing reactions have been proved to be inhibited by an excess of this metabolite *in vitro* (1). Moreover, even unrelated reactions are affected due to the

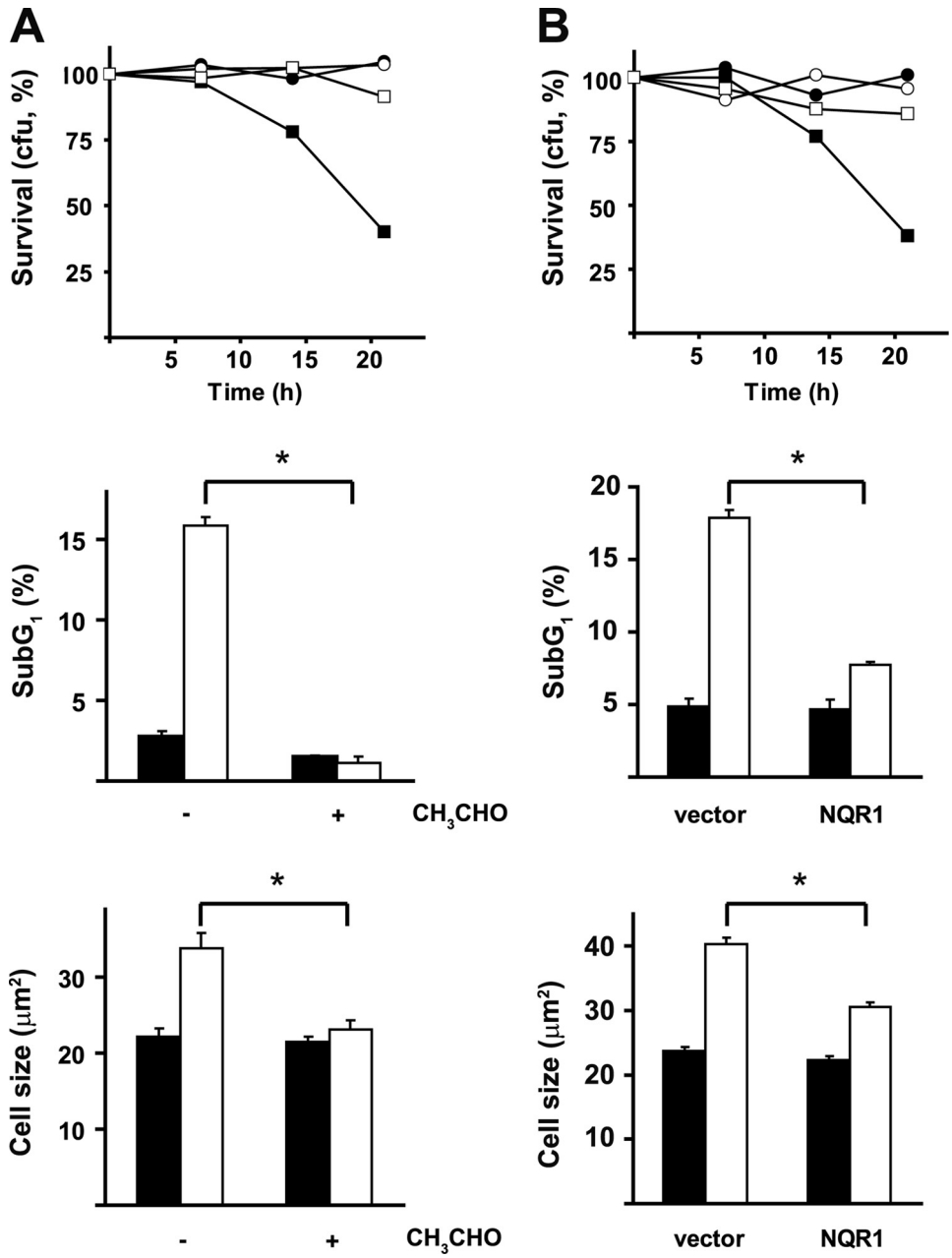

FIGURE 6. **NAD^+ homeostasis and cell death.** *A*, alteration of NAD^+ metabolism using acetaldehyde. YPC3 cells were incubated in the presence or absence of 10 mM acetaldehyde while kept under control (2% galactose; *solid bars*) or caloric restriction conditions (0.5% glucose; *open bars*). *Top panel*, ability to form individual colonies (cfu). *Open symbols*, galactose; *solid symbols*, CR; *squares*, wild-type control (YPC3); *circles*, acetaldehyde. The number of colonies representing 100% survival was 709 and 245 for untreated and acetaldehyde-treated control cells, respectively. A representative experiment is shown. *Middle panel*, proportion of cells showing DNA contents smaller than Gap 1 cells (sub-G_1) observed in propidium iodide FACS histograms with respect to the whole population (10,000 cells analyzed). *Bottom panel*, apparent cell size (area in μm^2) observed under the microscope. For *middle* and *bottom panels*, *solid bar*, galactose; *open bar*, CR. *B*, alteration of NAD^+ metabolism by overexpression of an alternative NADH oxidase. YPC3 cells carrying an empty expression vector (*vector*) or the plasma membrane-bound NADH coenzyme Q reductase 1 gene (*NQR1*) were placed under control (2% galactose; *solid bars*) or caloric restriction conditions (0.5% glucose; *open bars*). *Symbols* and experiments are the same as in *A*. The number of colonies representing 100% survival in the *middle panel* was 503 and 525 for YPC3 and NQR1 cells, respectively. Ten thousand cells per case were analyzed by flow cytometry. In all experiments, cells were incubated in glucose-containing medium for 18 h and kept at $A \leq 0.5$ prior to analysis. *Asterisks* denote significant statistical differences ($p \leq 0.05$). For all panels, *error bars* correspond to S.E. ($n = 3$).

side effects of attaining high concentrations of PP_i, such as sequestration of Mg^{2+} ions (1), making elimination of excess PP_i a critical issue in cell metabolism. In this regard, the nicotinic acid-mononucleotide adenylyltransferase step in the biosynthesis of NAD^+ was the first major biochemical reaction described both to produce this metabolite and to be inhibited by it (35). Other PP_i-producing biological reactions are also affected by an excess of PP_i, for example, the polymerization of macromolecules, such as proteins, RNA, and DNA. However, despite an important and still open discussion on the influence of PP_i levels on the fidelity of nucleotide or amino acid incorporation into macromolecules (40, 41), it is unknown whether any of them are especially sensitive to excess PP_i and therefore candidates for the growth defects observed in bacteria and

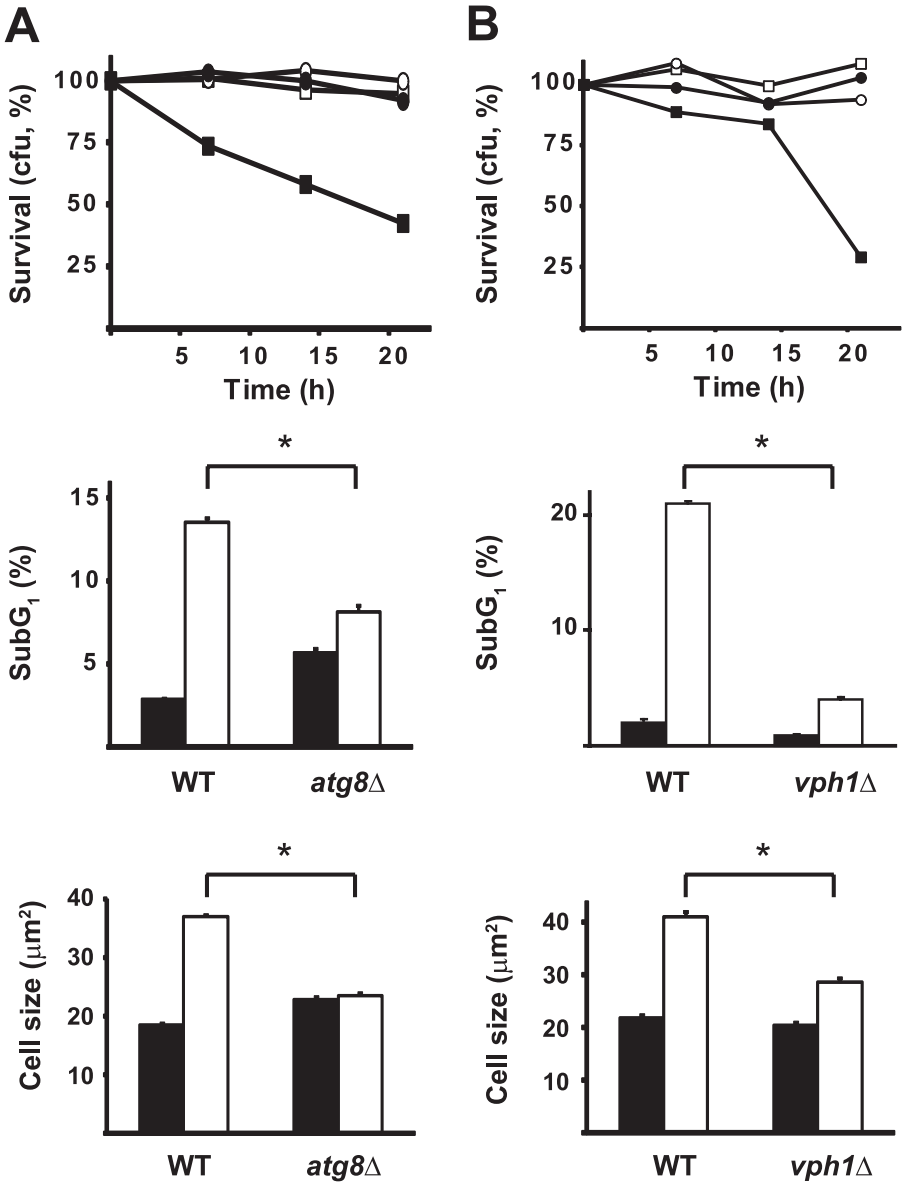

FIGURE 7. **Effect of autophagy deficiency on cell death.** *A*, effect of a mutation in the early steps of autophagy. Wild-type and mutant *atg8*Δ strains correspond to SAH16 and SAH17, respectively ("Experimental Procedures"). *Top panel*, ability to form individual colonies (cfu). *Open symbols*, galactose; *solid symbols*, SG; *squares*, wild-type strain; *circles*, *atg8*Δ. The number of colonies representing 100% survival was 198 and 187 for wild-type and *atg8*Δ strains grown under control conditions, respectively. A representative experiment is shown. *Middle panel*, proportion of cells showing sub-G_1 DNA contents with respect to the whole population (10,000 cells analyzed). *Bottom panel*, apparent cell size (area in μm^2). For *middle* and *bottom panels*, *solid bars*, galactose; *open bars*, SG. *B*, effect of a blockage in the late steps of autophagy. Mutant *vph1*Δ was constructed on a YPC3 background, and the latter is used as a wild-type strain ("Experimental Procedures"). *Symbols* and experiments are the same as in *A*. The number of colonies representing 100% survival in the *top panel* was 709 and 789 for YPC3 and *vph1*Δ cells, respectively. In all experiments, cells were incubated in glucose-containing medium for 18 h and kept at $A \leq 0.5$ prior to analysis. *Asterisks* denote significant statistical differences ($p \leq 0.05$). For all panels, *error bars* correspond to S.E. ($n = 3$).

yeast. As we show in the present work, under some conditions, one of the cellular processes most sensitive to excess PP_i seems to be the homeostasis of nicotinamide.

In yeast, fermentation places cells in a delicate redox equilibrium. On the one hand, nicotinamide coenzyme concentrations are low ([NAD^+] + [NADH] is approximately 1 mM), and as a result, most of the cytosolic coenzyme is probably committed to cycle between its oxidized and reduced forms in glycolysis. On the other, this process is stoichiometrically rigid; *i.e.* the capacity to oxidize NADH by acetaldehyde reduction using alcohol dehydrogenase is equivalent to the amount that was previously reduced by the glyceraldehyde-3-phosphate dehydrogenase, and thus, the cell lacks any flexibility to alter its NAD^+/NADH ratio through metabolism. This means that any further needs for NAD^+ must be covered by biosynthesis of new coenzyme molecules. It is noteworthy that in the cell there are several reactions that consume NAD^+ and eventually destroy it, *e.g.* ADP-ribose transferases, cADP-ribose synthases, sirtuins, and in the case of mammals poly(ADP-ribose) polymerases. At least in mammals, under some conditions, such as DNA damage by genotoxic drugs, these processes can even deplete cellular NAD^+ contents (42). Both known pathways for NAD^+ biosynthesis, salvage and *de novo* biosynthesis, include steps where PP_i is formed and hence where an excess of this compound can act

as an effective inhibitor. Noticeably, the rate-limiting step in NAD^+ biosynthesis, shared by both *de novo* and salvage pathways, is the adenylation of nicotinic acid mononucleotide, a reversible reaction among the first ones described to be sensitive to excess PP_i (1, 35). In addition, the transfer of a phosphoribosyl moiety to yield nicotinamide/nicotinic acid mononucleotide and PP_i in the salvage pathway is also reversible (43). The salvage pathway is considered the primary pathway for NAD^+ synthesis in yeast (44). Which of these steps is primarily responsible for the observed cell death induction in fermenting cells is still unknown. Research on this subject may offer a potential way to control cell proliferation.

Caloric restriction has been shown to lengthen lifespan and affect many cellular processes in nearly all living model systems with the exception of plants (44). The best accepted mechanism relies on the increase of the concentration of NAD^+ at the expense of NADH. Sirtuins, NAD^+-dependent histone deacetylases, are derepressed by a relative excess of NAD^+, and gene expression is altered through transcriptional silencing, resulting in changes in lifespan. In yeast, the presence of glucose at a low concentration (typically 0.5%) is enough to induce a mixed metabolism comprising fermentation and respiration that helps maintaining a high NAD^+/NADH ratio and increase lifespan (45, 46). In the case of cytosolic sPPase depletion, we have shown that increasing NAD^+ availability in the cell inhibited the induction of autophagy and cell death. Despite this, caloric restriction could not increase survival, extent of cell death induction, or its time course. Noticeably, overexpression of an alternative NADH oxidase, such as Nqr1p, was only able to alleviate cell death under caloric restriction conditions. This suggests that nicotinamide coenzyme homeostasis must be sternly pushed toward NAD^+ production or NADH reoxidation (*e.g.* addition of high concentrations of acetaldehyde) to alleviate cell death effectively and that milder strategies, such as caloric restriction and Nqr1p overexpression, are only effective when in combination.

Although cell death is usually accompanied by prior cell cycle arrest, a general inhibitory effect of anabolism by excess PP_i could be perfectly understood with an asynchronous arrest of cell functions. Our data show that under both fermentative (SG and CR) and respiratory (MR) conditions cell cycle arrest is part of the cellular responses to cytosolic sPPase depletion. In the case of fermentative conditions, G_0/G_1 arrest is observed. This could be a response to a deficiency in nicotinamide coenzymes. Subsequent induction of autophagy seems to reinforce this idea. In the case of cells maintained in glycerol as a carbon source, an S phase arrest may suggest that DNA duplication together with nicotinamide coenzyme biosynthesis is one of the biochemical processes most sensitive to an excess of PP_i in the cell. Further work is being carried out in our laboratory to shed light on this topic.

All in all, the present report constitutes the first cell physiology study on the alteration of PP_i homeostasis in eukaryotes in terms of its effects on cell cycle and cell death induction. These data have clear importance to understand which processes are most likely affected by an excess of cellular PP_i and may also be useful to design new alternative therapeutic approaches against diseases like cancer or bone disorders.

Acknowledgments—We thank Dr C. Santos-Ocaña for the gift of the NQR1 expression plasmid and together with Dr. R. Wellinger for helpful discussions. We also thank I. Jiménez for invaluable technical assistance.

REFERENCES

1. Heinonen, J. K. (2001) *Biological Role of Inorganic Pyrophosphate*, Kluwer Academic Publishers, Dordrecht, Netherlands
2. Pérez-Castiñeira, J. R., Gómez-García, R., López-Marqués, R. L., Losada, M., and Serrano, A. (2001) Enzymatic systems of inorganic pyrophosphate bioenergetics in photosynthetic and heterotrophic protists: remnants or metabolic cornerstones? *Int. Microbiol.* **4,** 135–142
3. Serrano, A., Pérez-Castiñeira, J. R., Baltscheffsky, M., and Baltscheffsky, H. (2007) H^+-PPases: yesterday, today and tomorrow. *IUBMB Life* **59,** 76–83
4. Chen, J., Brevet, A., Fromant, M., Lévêque, F., Schmitter, J.-M., Blanquet, S., and Plateau, P. (1990) Pyrophosphatase is essential for growth of *Escherichia coli*. *J. Bacteriol.* **172,** 5686–5689
5. Ben-Aroya, S., Coombes, C., Kwok, T., O'Donnell, K. A., Boeke, J. D., and Hieter, P. (2008) Toward a comprehensive temperature-sensitive mutant repository of the essential genes of *Saccharomyces cerevisiae*. *Mol. Cell* **30,** 248–258
6. Breslow, D. K., Cameron, D. M., Collins, S. R., Schuldiner, M., Stewart-Ornstein, J., Newman, H. W., Braun, S., Madhani, H. D., Krogan, N. J., and Weissman, J. S. (2008) A comprehensive strategy enabling high-resolution functional analysis of the yeast genome. *Nat. Methods* **5,** 711–718
7. Giaever, G., Chu, A. M., Ni, L., Connelly, C., Riles, L., Véronneau, S., Dow, S., Lucau-Danila, A., Anderson, K., André, B., Arkin, A. P., Astromoff, A., El-Bakkoury, M., Bangham, R., Benito, R., Brachat, S., Campanaro, S., Curtiss, M., Davis, K., Deutschbauer, A., Entian, K. D., Flaherty, P., Foury, F., Garfinkel, D. J., Gerstein, M., Gotte, D., Güldener, U., Hegemann, J. H., Hempel, S., Herman, Z., Jaramillo, D. F., Kelly, D. E., Kelly, S. L., Kötter, P., LaBonte, D., Lamb, D. C., Lan, N., Liang, H., Liao, H., Liu, L., Luo, C., Lussier, M., Mao, R., Menard, P., Ooi, S. L., Revuelta, J. L., Roberts, C. J., Rose, M., Ross-Macdonald, P., Scherens, B., Schimmack, G., Shafer, B., Shoemaker, D. D., Sookhai-Mahadeo, S., Storms, R. K., Strathern, J. N., Valle, G., Voet, M., Volckaert, G., Wang, C. Y., Ward, T. R., Wilhelmy, J., Winzeler, E. A., Yang, Y., Yen, G., Youngman, E., Yu, K., Bussey, H., Boeke, J. D., Snyder, M., Philippsen, P., Davis, R. W., and Johnston, M. (2002) Functional profiling of the *Saccharomyces cerevisiae* genome. *Nature* **418,** 387–391
8. Pérez-Castiñeira, J. R., López-Marqués, R. L., Villalba, J. M., Losada, M., and Serrano, A. (2002) Functional complementation of yeast cytosolic pyrophosphatase by bacterial and plant H^+-translocating pyrophosphatases. *Proc. Natl. Acad. Sci. U.S.A.* **99,** 15914–15919
9. Kukko-Kalske, E., Lintunen, M., Inen, M. K., Lahti, R., and Heinonen, J. (1989) Intracellular PPi concentration is not directly dependent on amount of inorganic pyrophosphatase in *Escherichia coli* K-12 cells. *J. Bacteriol.* **171,** 4498–4500
10. Polewski, M. D., Johnson, K. A., Foster, M., Millán, J. L., and Terkeltaub, R. (2010) Inorganic pyrophosphatase induces type I collagen in osteoblasts. *Bone* **46,** 81–90
11. Weissen-Plenz, G., Nitschke, Y., and Rutsch, F. (2008) Mechanisms of arterial calcification: spotlight on the inhibitors. *Adv. Clin. Chem.* **46,** 263–293
12. Chen, G., Gharib, T. G., Huang, C.-C., Thomas, D. G., Shedden, K. A., Taylor, J. M., Kardia, S. L., Misek, D. E., Giordano, T. J., Iannettoni, M. D., Orringer, M. B., Hanash, S. M., and Beer, D. G. (2002) Proteomic analysis of lung adenocarcinoma: identification of a highly expressed set of proteins in tumors. *Clin. Cancer Res.* **8,** 2298–2305
13. Tomonaga, T., Matsushita, K., Yamaguchi, S., Oh-Ishi, M., Kodera, Y., Maeda, T., Shimada, H., Ochiai, T., and Nomura, F. (2004) Identification of altered protein expression and post-translational modifications in primary colorectal cancer by using agarose two-dimensional gel electrophoresis. *Clin. Cancer Res.* **10,** 2007–2014
14. Gómez-García, M. R., Losada, M., and Serrano, A. (2006) A novel subfam-

ily of monomeric inorganic pyrophosphatases in photosynthetic eukaryotes. *Biochem. J.* **395,** 211–221
15. Geigenberger, P., Hajirezaei, M., Geiger, M., Deiting, U., Sonnewald, U., and Stitt, M. (1998) Overexpression of pyrophosphatase leads to increased sucrose degradation and starch synthesis, increased activities of enzymes for sucrose-starch interconversions, and increased levels of nucleotides in growing potato tubers. *Planta* **205,** 428–437
16. George, G. M., van der Merwe, M. J., Nunes-Nesi, A., Bauer, R., Fernie, A. R., Kossmann, J., and Lloyd, J. R. (2010) Virus-induced gene silencing of plastidial soluble inorganic pyrophosphatase impairs essential leaf anabolic pathways and reduces drought stress tolerance in *Nicotiana benthamiana*. *Plant Physiol.* **154,** 55–66
17. Sonnewald, U. (1992) Expression of *E. coli* inorganic pyrophosphatase in transgenic plants alters photoassimilate partitioning. *Plant J.* **2,** 571–581
18. Drake, R., Serrano, A., and Pérez-Castiñeira, J. R. (2010) N-terminal chimaeras with signal sequences enhance the functional expression and alter the subcellular localization of heterologous membrane-bound inorganic pyrophosphatases in yeast. *Biochem. J.* **426,** 147–157
19. Jiménez-Hidalgo, M., Santos-Ocaña, C., Padilla, S., Villalba, J. M., López-Lluch, G., Martín-Montalvo, A., Minor, R. K., Sinclair, D. A., de Cabo, R., and Navas, P. (2009) NQR1 controls lifespan by regulating the promotion of respiratory metabolism in yeast. *Aging Cell* **8,** 140–151
20. Gietz, R. D., and Woods, R. A. (2002) Transformation of yeast by lithium acetate/single-stranded carrier DNA/polyethylene glycol method. *Methods Enzymol.* **350,** 87–96
21. Wlodkowic, D., Skommer, J., and Darzynkiewicz, Z. (2009) Flow cytometry-based apoptosis detection. *Methods Mol. Biol.* **559,** 19–32
22. Sazer, S., and Sherwood, S. W. (1990) Mitochondrial growth and DNA synthesis occur in the absence of nuclear DNA replication in fission yeast. *J. Cell Sci.* **97,** 509–516
23. Hernández, A., López-Lluch, G., Navas, P., and Pintor-Toro, J. A. (2009) HDAC and Hsp90 inhibitors down-regulate PTTG1/securin but do not induce aneuploidy. *Genes Chromosomes Cancer* **48,** 194–201
24. Collins, T. J. (2007) ImageJ for microscopy. *Biotechniques* **43,** (suppl.) 25–30
25. Madeo, F., Fröhlich, E., and Fröhlich, K. U. (1997) A yeast mutant showing diagnostic markers of early and late apoptosis. *J. Cell Biol.* **139,** 729–734
26. Journo, D., Winter, G., and Abeliovich, H. (2008) Monitoring autophagy in yeast using FM 4-64 fluorescence. *Methods Enzymol.* **451,** 79–88
27. Rathbun, W. B., and Betlach, M. V. (1969) Estimation of enzymically produced orthophosphate in the presence of cysteine and adenosine triphosphate. *Anal. Biochem.* **28,** 436–445
28. Collart, M. A., and Oliviero, S. (2001) Preparation of yeast RNA. *Curr. Protoc. Mol. Biol.* **Chapter 13,** Unit 13.12
29. Carroll, A. S., and O'Shea, E. K. (2002) Pho85 and signaling environmental conditions. *Trends Biochem. Sci.* **27,** 87–93
30. Verstrepen, K. J., Iserentant, D., Malcorps, P., Derdelinckx, G., Van Dijck, P., Winderickx, J., Pretorius, I. S., Thevelein, J. M., and Delvaux, F. R. (2004) Glucose and sucrose: hazardous fast-food for industrial yeast? *Trends Biotechnol.* **22,** 531–537
31. Wilkinson, S., and Ryan, K. M. (2010) Autophagy: an adaptable modifier of tumourigenesis. *Curr. Opin. Genet. Dev.* **20,** 57–64
32. Zuin, A., Castellano-Esteve, D., Ayté, J., and Hidalgo, E. (2010) Living on the edge: stress and activation of stress responses promote lifespan extension. *Aging* **2,** 231–237
33. Johnston, M., Flick, J. S., and Pexton, T. (1994) Multiple mechanisms provide rapid and stringent glucose repression of GAL gene expression in *Saccharomyces cerevisiae*. *Mol. Cell. Biol.* **14,** 3834–3841
34. Ruckenstuhl, C., Carmona-Gutierrez, D., and Madeo, F. (2010) The sweet taste of death: glucose triggers apoptosis during yeast chronological aging. *Aging* **2,** 643–649
35. Kornberg, A., and Pricer, W. E., Jr. (1950) Nucleotide pyrophosphatase. *J. Biol. Chem.* **182,** 763–778
36. Billington, R. A., Genazzani, A. A., Travelli, C., and Condorelli, F. (2008) NAD depletion by FK866 induces autophagy. *Autophagy* **4,** 385–387
37. Portt, L., Norman, G., Clapp, C., Greenwood, M., and Greenwood, M. T. (2011) Anti-apoptosis and cell survival: a review. *Biochim. Biophys. Acta* **1813,** 238–259
38. Kim, J., Huang, W. P., and Klionsky, D. J. (2001) Membrane recruitment of Aut7p in the autophagy and cytoplasm to vacuole targeting pathways requires Aut1p, Aut2p, and the autophagy conjugation complex. *J. Cell Biol.* **152,** 51–64
39. Nakamura, N., Matsuura, A., Wada, Y., and Ohsumi, Y. (1997) Acidification of vacuoles is required for autophagic degradation in the yeast, *Saccharomyces cerevisiae*. *J. Biochem.* **121,** 338–344
40. Batabyal, D., McKenzie, J. L., and Johnson, K. A. (2010) Role of histidine 932 of the human mitochondrial DNA polymerase in nucleotide discrimination and inherited disease. *J. Biol. Chem.* **285,** 34191–34201
41. Wolfson, A. D., and Uhlenbeck, O. C. (2002) Modulation of tRNAAla identity by inorganic pyrophosphatase. *Proc. Natl. Acad. Sci. U.S.A.* **99,** 5965–5970
42. Kirkland, J. B. (2010) Poly ADP-ribose polymerase-1 and health. *Exp. Biol. Med.* **235,** 561–568
43. Takahashi, R., Nakamura, S., Nakazawa, T., Minoura, K., Yoshida, T., Nishi, Y., Kobayashi, Y., and Ohkubo, T. (2010) Structure and reaction mechanism of human nicotinamide phosphoribosyltransferase. *J. Biochem.* **147,** 95–107
44. Lu, S.-P., and Lin, S.-J. (2010) Regulation of yeast sirtuins by NAD(+) metabolism and calorie restriction. *Biochim. Biophys. Acta* **1804,** 1567–1575
45. Lin, S.-J., Ford, E., Haigis, M., Liszt, G., and Guarente, L. (2004) Calorie restriction extends yeast life span by lowering the level of NADH. *Genes Dev.* **18,** 12–16
46. Lin, S.-J., Kaeberlein, M., Andalis, A. A., Sturtz, L. A., Defossez, P.-A., Culotta, V. C., Fink, G. R., and Guarente, L. (2002) Calorie restriction extends *Saccharomyces cerevisiae* lifespan by increasing respiration. *Nature* **418,** 344–348